CORA Cork Open Research Archive
Cartlann Taighde Oscailte Chorcaí

| | |
|---|---|
| Title | Multiplicative time and space integrating acousto-optic architectures for real time spectrum processing |
| Authors | Riza, Nabeel A.;Psaltis, Demetri |
| Publication date | 1987-11-25 |
| Original Citation | Riza, N. A. and Psaltis, D. (1987) 'Multiplicative Time And Space Integrating Acousto-Optic Architectures For Real Time Spectrum Processing', Proceedings of SPIE, 0827, Real-Time Signal Processing X, 31st Annual Technical Symposium on Optical and Optoelectronic Applied Sciences and Engineering, 1987, San Diego, CA, United States, 25 November, doi: 10.1117/12.942069 |
| Type of publication | Conference item |
| Link to publisher's version | 10.1117/12.942069 |
| Rights | © 1987 Society of Photo-Optical Instrumentation Engineers (SPIE). One print or electronic copy may be made for personal use only. Systematic reproduction and distribution, duplication of any material in this paper for a fee or for commercial purposes, or modification of the content of the paper are prohibited. |
| Download date | 2026-10-31 15:25:26 |
| Item downloaded from | https://hdl.handle.net/10468/10137 |



UCC
University College Cork, Ireland
Coláiste na hOllscoile Corcaigh

PROCEEDINGS OF SPIE

SPIEDigitalLibrary.org/conference-proceedings-of-spie

# Multiplicative Time And Space Integrating Acousto-Optic Architectures For Real Time Spectrum Processing

Riza, Nabeel, Psaltis, Demetri

Nabeel A. Riza, Demetri Psaltis, "Multiplicative Time And Space Integrating Acousto-Optic Architectures For Real Time Spectrum Processing," Proc. SPIE 0827, Real-Time Signal Processing X, (25 November 1987); doi: 10.1117/12.942069

SPIE.

Event: 31st Annual Technical Symposium on Optical and Optoelectronic Applied Sciences and Engineering, 1987, San Diego, CA, United States

Downloaded From: https://www.spiedigitallibrary.org/conference-proceedings-of-spie on 07 Jun 2020 Terms of Use: https://www.spiedigitallibrary.org/terms-of-use

# Multiplicative Time and Space Integrating Acousto-optic Architectures for Real Time Spectrum Processing

**Nabeel A. Riza and Demetri Psaltis**

**Department of Electrical Engineering**
**California Institute of Technology**
**Pasadena, CA 91125**

## Abstract

Multiplicative acousto-optic architectures using time and space dimensions for spectrally resolving long 1-D signals and images are described. The Discrete Fourier Transform algorithm is implemented optically to provide fine frequency resolving power. Experimental results are presented for 1-D and 2-D input signals. Bias removal techniques are discussed, including an approach using a photorefractive crystal as a time integrating bias-free detector.

## 1. Introduction

This paper describes multiplicative time and space integrating (TSI) acousto-optic architectures for spectrum analysis of images and long 1-D signals. The TSI approach is used which combines the best features of 1-D space integrating and 1-D time integrating spectrum analyzers.[1,2] Wagner and Psaltis have previously demonstrated experimentally an additive architecture for folded spectrum processing of 1-D signals.[3,4] In this paper we describe and experimentally demonstrate a multiplicative processor suitable for finding the 2-D Fourier spectrum of images. The information signal is fed into a Bragg cell and a lens takes the Fourier transform in the coarse frequency (x) direction of the image. In the second orthogonally oriented Bragg cell, the DFT signal is entered which along with the time integrating CCD calculates the Fourier transform in the fine frequency (y) direction of the image. We begin the paper by describing the principles of TSI processing. The space integrating spectrum analyzer is described using 1-D time signals and 2-D video images as inputs. Then, the Discrete Fourier transform (DFT) based time integrating spectrum analyzer is described and experimental results are given. The possible TSI architecture is given and analysis is carried out. Experimental data is presented and system performance issues such as bias removal techniques are discussed. We end with a summary of the processor and its possible applications.

## 2. Space Integrating Spectrum Analyzer

Fig. 1 shows the optical setup for the SI Spectrum Analyzer. The field amplitude at the detector plane is

$$\begin{aligned} F(x',t) &= \int_A \tilde{s}(t-\frac{x}{v}) e^{-j2\pi x \frac{x'}{\lambda F}} dx\, e^{-j\omega t} \\ &= [v\tilde{S}(uv) e^{-j2\pi uvt} * Asinc(Au)]\, e^{-j\omega t} \end{aligned}$$

where $v$ is the acoustic signal velocity in the Bragg cell and $\tilde{s}(t)$ is the diffracted signal where

$$s(t) = 0.5[\tilde{s}(t) + \tilde{s}^*(t)]$$

Using a reference signal $r$ for hetrodyne detection, the intensity on the detector plane can be written as

$$I(x',t) = |[v\tilde{S}(uv) e^{-j2\pi vut} * B(u)] + r|^2$$

where $B(u)$ is the blurr spot taking into account the finite aperture of the Bragg cell and acoustic apodization effects. Note that the reference signal can be introduced by either electronic or optical means. In the processor to be described, we use an electronic reference, in particular, a high bandwidth periodic chirp signal that is electronically added to the input signal before being input to the Bragg cell. This chirp has a period corresponding to the laser diode pulse rate and is phase reset every light pulse. In the Fourier plane, the signal and chirp spectra add together optically, thus retaining the phase information in the input signal. For a single tone input

$$s(t) = a\cos(2\pi f' t)$$

the intensity is

$$I(x',t) = |a|^2 B^2(u - \frac{f'}{v}) + |r|^2 + 2|a|rB(u - \frac{f'}{v})\cos(2\pi f' t + \Omega)$$



Downloaded From: https://www.spiedigitallibrary.org/conference-proceedings-of-spie on 07 Jun 2020
Terms of Use: https://www.spiedigitallibrary.org/terms-of-use

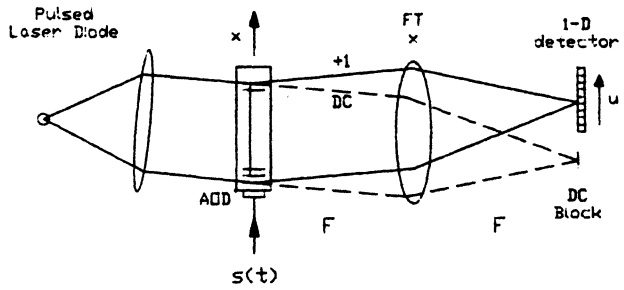



**Fig. 1** Space Integrating Spectrum Analyzer

where $r$ corressponds to the reference chirp spectrum in the Fourier plane. Taking the pulsing action of the laser diode into account every T seconds where the trigger pulse train is approximated in the limit as a impulse train, the intensity on the $n^{th}$ pulse is

$$I(x', n) = |a|^2 B^2(u - \frac{f_c}{v}) + |r|^2 + 2|a|rB(u - \frac{f_c}{v}) \cos(2\pi\delta nT + \Omega) \tag{1}$$

where

$$f' == f_c + \delta$$

$$f_c = \frac{k}{T}$$

$$a = |a|e^{j\Omega}.$$

Eqn. 1 shows that for a single tone input, the output of the processor consists of a constant bias, a signal dependent bias term positioned according to the signal coarse frequency $f_c$, and a sampled temporal modulation at the signal fine frequency. The third term contains the original input signal, except it has been heterodyned to baseband by the pulsing action of the laser diode. It is this temporal modulation that allows us to use time domain spectral analysis schemes, such as the DFT algorithm to resolve the signal into higher resolution spectral components. In order to avoid aliasing effects between the bandlimited signals in each coarse frequency blurr spot,we need to satisfy the Nyquist criteria .i.e

$$\frac{1}{T} > \frac{2}{T_a}$$

where T is the sampling time of the laser diode and $T_a$ is the aperture of the Bragg cell.

When $s(t)$ is a video signal where $f_n(x)$ represents the $n^{th}$ video line, the field amplitude at the detector plane can be written as

$$E(u, n) \approx K[\tilde{F}_n(u) * B(u)] \tag{2}$$

where $K$ is a scaling factor. For a camera looking at a tilted grating image with a spatial frequency $u_0$ in the x coordinate direction (fast temporal variation) and frequency $v_0$ in the y (slow) direction,

$$f_n(x) = \cos[2\pi(u_0 x + v_0 n\Delta y)]$$

$$u_0 \geq \frac{1}{vT_v}$$

where $T_v$ is the video line time. In this mode of system operation, the laser diode pulsing rate should be set equal to the video line rate.i.e. $T = T_v$ For example, if we have a grating with variation only in the x direction, ( $v_0 = 0$), from Eqn. 2 we get

$$E(u, n) = K[B(u - u_0) + B(u + u_0)] \tag{3}$$

and for a variation only in the y direction of the image,

$$E(u, n) \approx KB(u) \cos(2\pi v_{,,} n\Delta y) \tag{4}$$

From Eqn. 3 it is clear that the spatial frequencies along the x direction of an image can be resolved in the Fourier plane by using an acousto-optic device as an input transducer and a Fourier transforming lens to spatially



Downloaded From: https://www.spiedigitallibrary.org/conference-proceedings-of-spie on 07 Jun 2020
Terms of Use: https://www.spiedigitallibrary.org/terms-of-use

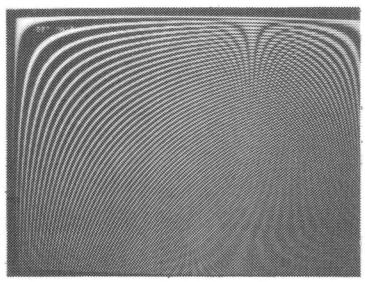


**Fig. 2** DFT Signal Stored in a Computer

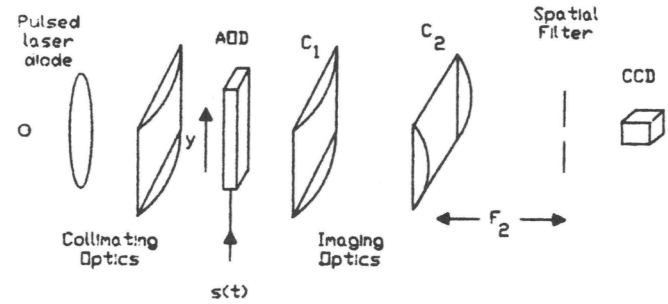



**Fig. 3** Time Integrating Spectrum Analyzer

channelize these frequencies into frequency bins. Eqn. 4 tells us that spatial variations of frequency $v_0$ along the y direction in the image are converted by the pulsing space integrating acousto-optic spectrum analyzer to a sampled temporal variation of the same frequency. This temporal variation can then be channelized into its frequency bins along the y direction by using time integration as we will describe in the next section.

## 3. Time Integrating Spectrum Analyzer Experiment

We use the DFT algorithm to implement the time integrating portion of the spectrum analysis.[5,6] The DFT of a sequence s(n) is described by

$$S(k) = \sum_{n=0}^{n=N-1} s(n) {W_N}^{nk}$$

$$W_N = e^{-j\frac{2\pi}{N}} .$$

This operation can be broken up into a summation over n of the products of the input signal samples with its corressponding DFT matrix elements. As the DFT matrix is symmetric, we require only half the terms in a DFT column. Each column is a sinusoid with an additional half cycle for each subsequent DFT column. The signal $d(t)$ that is applied to the acousto-optic device through which the DFT signal is introduced, is given by:

$$d(t) = \sum_{n=0}^{N-1} \cos[n\Delta\omega(t - nT)] rect[\frac{t - nT}{T}] . \tag{5}$$

A personal computer was used to generate the DFT signal. The DFT signal is stored in a 2-D raster format in a computer and it is displayed in Fig. 2. This method calculates the cosine transform i.e. the real part of the complex fourier spectrum. Fig. 3 shows the laboratory set up for the implementation of the DFT, time integrating spectrum analyzer. The laser diode is pulsed at the video line rate and the input signal $s(t)$ into the Bragg cell is

$$s(t) = \cos[(\omega_0 + \delta)t] + d(t)\cos\omega_0 t ,$$

where $\omega_0$ is the center frequency of the Bragg cell. The light diffracted by the Bragg cell is imaged on to the CCD with appropriate single sideband filtering done in the Fourier plane of cylinderical lens $C_2$. The light intensity integrated on the CCD is

$$I(y) = \sum_{n=0}^{n=N-1} |e^{-j(\omega_0+\delta)(nT-\frac{y}{v})} + \frac{1}{4} e^{-j[\omega_0(nT-\frac{y}{v})+n\frac{\Delta\omega}{v}y]}|^2$$

$$I(y) \approx C + \cos(\frac{\omega_s}{v}y + \beta)\frac{\sin(N\alpha)}{\sin\alpha}$$

where

$$\alpha = \frac{1}{2}(\delta T - \frac{\Delta\omega}{v}y)$$

$\omega_s$ and $\beta$ are signal dependent spatial frequency and phase terms and $C$ is constant bias term. A typical value for $\omega_s$ is $\approx$ 1.86 cycles per mm which gives only a few cycles on the CCD surface giving a very low modulation. Therefore, we see peaks located at the sinc type function maximum position $y = \frac{\delta T v}{\Delta\omega}$ corressponding to the signal



Downloaded From: https://www.spiedigitallibrary.org/conference-proceedings-of-spie on 07 Jun 2020
Terms of Use: https://www.spiedigitallibrary.org/terms-of-use

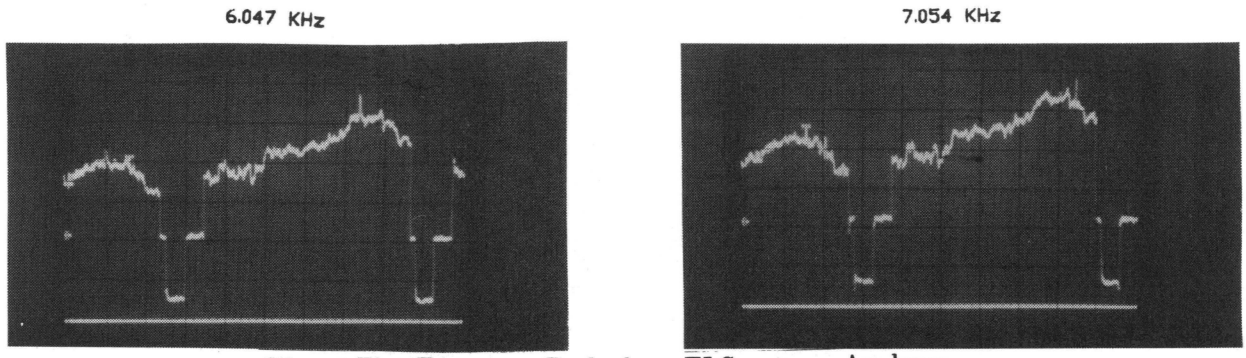



**Fig. 4** Fine Frequency Peaks from TI Spectrum Analyzer before Bias Subtraction

fine frequency $\delta$. In our experiment, $\delta$ is varied from DC to 7.8 KHz which corressponds to the bandwidth of a video image along its vertical $(y)$ or slower direction. Fig. 4 shows the experimental results before bias removal. The peak moves along the imaged DFT signal ridge with changing fine frequency.

## 4. Architecture for TSI Spectrum Analysis

Fig. 5 shows the TSI architecture for spectrum analysis using crossed Bragg cells , imaging optics, a pulsing laser diode , a CCD detector array and supplementary electronics. The signal chain for the system is as follows. The DFT signal $d(t)$ is added to a reference bias $a$ and it is mixed up to the center frequency $\omega_0$ of the Bragg cell before being used as the input to the acousto-optic device. This composite signal $s_1(t-\frac{x}{v})$ is then imaged on to the CCD plane with appropriate single sideband spatial filtering. In the other orthogonal Bragg cell,we enter the sum of a reference chirp $c(t)$ with the information signal $v(t)$ that has been mixed to the Bragg cell center frequency. A lens takes the Fourier transform of the signal $s_2(t)$ in the AO device and this spectrum is made to coincide with the detector plane. The electric field incident on the CCD detector plane is

$$E = [\int_A \tilde{s}_1(t-\frac{x}{v})e^{-j2\pi ux}dx][\tilde{s}_2(t+\frac{y}{v})]$$

where

$$s_1(t) = [v(t)+c(t)]\cos\omega_0 t$$
$$s_2(t) = [a+d(t)]\cos\omega_0 t$$
$$v(t) = \sum_{n=0}^{n=N-1} f_n(t-nT)rect(\frac{t-nT}{T})$$

for a video signal.

$$c(t) = \sum_{n=0}^{n=N-1} \cos[b(t-nT)^2]rect(\frac{t-nT}{T})$$

and $d(t)$ is defined in Eqn. 5. Taking into account the pulsing of the laser diode and the single sideband filtering, we get the intensity due to the $n_{th}$ pulse as

$$|E_n|^2 \approx |[v(\tilde{F}_n(vu)+\tilde{C}(vu)) * AsincAu][a+e^{-jn\frac{\Delta\omega}{v}y}]|^2 \quad (6)$$

On expanding Eqn. 6 (see appendix A), and collecting similar terms, we get the total time integrated interferometrically generated charge distribution recorded on the CCD after a frame time to be as follows:

$$I(u,y) = KRe[\sum_{n=0}^{n=N-1}(\tilde{F}_n(u) * B(u))\cos(n\frac{\Delta\omega}{v}y)] + K_1 + K_2 \quad (7)$$

where the first term gives the 2-D Cosine transform of the input signal and $K_1$ and $K_2$ represent constant bias and signal dependent bias terms respectively. $K$ is a scaling constant and we have assumed that the reference chirp spectrum is uniform over the bandwidth of the information signal. The blurr spot $B(u)$ has been used in the analysis.



Downloaded From: https://www.spiedigitallibrary.org/conference-proceedings-of-spie on 07 Jun 2020
Terms of Use: https://www.spiedigitallibrary.org/terms-of-use

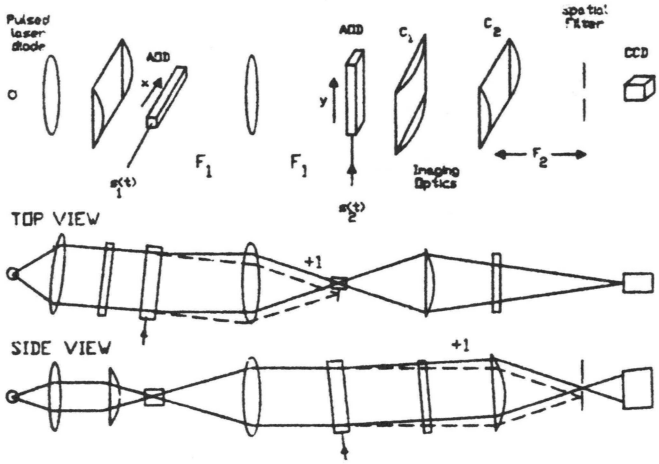



**Fig. 5** TSI Spectrum Analyzer using Cylinders for Imaging

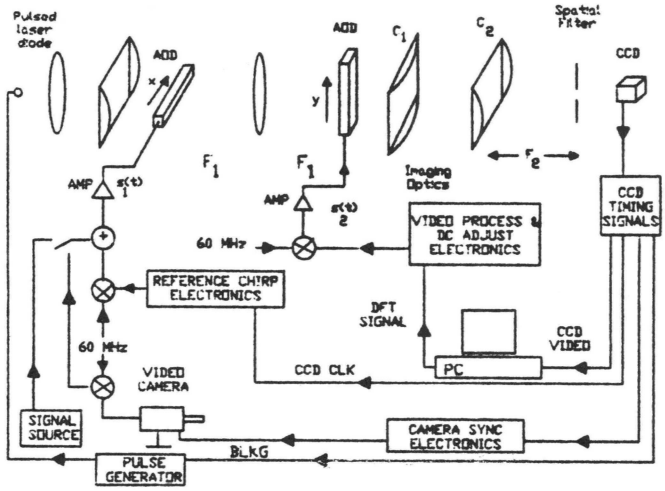



**Fig. 6** Laboratory Setup of TSI System

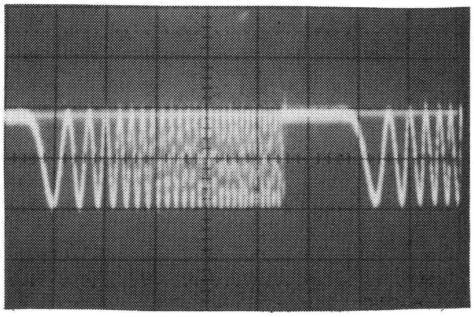


**Fig. 7(a)** PROM Generated Reference Chirp

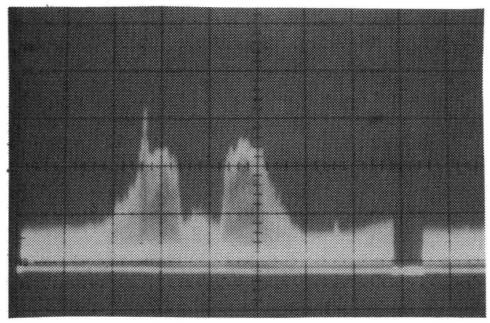


**Fig. 7(b)** Fourier Plane Spectra of a 3 MHz Input Tone and 3.5 MHz Reference Chirp

For a continous time signal as input, the first term of eqn. 7 represents the folded spectrum of the input. On the otherhand,for a video signal input, it gives the 2-D video image spectrum. See appendix A for the impulse response of the system corressponding to the two types of input. The architecture in Fig. 5 uses crossed cylinders for imaging. This imaging method gives lens values that assure overall short system length and desired demagnifications for compatibility with the CCD detector specifications. In our case, we used 10 cm and 15 cm cylinderical lenses to achieve the desired demagnifications.

Fig. 6 shows the laboratory setup of the architecture in Fig. 5. The system timing is controlled by the CCD detector 7.16 MHz internal oscillator. The CCD blanking signal is used to generate a 15.734 KHz laser diode trigger signal with a pulse width of 100 nsec. This corressponds to a light flash every video line time. The anamorphic gaussian beam profile of the laser diode is collimated by the spherical lens such that the long axis is along the x direction of the SI AOD aperture. The Bragg diffracted light from the first AOD is Fourier transformed by a spherical lens in the x direction and recollimated in the y direction giving a slit of light positioned in the aperture of the second AOD. The Bragg diffracted light from the second AOD is imaged on to the CCD using the crossed cylinders. In the Fourier plane of the cylinder with power in the y direction, the appropriate spatial single sideband filtering is done. The AOD's used in this experiment are slow shear mode Telirium Dioxide devices with an aperture time of 70 $\mu sec$ and bandwidth of 40 MHz. A 60 MHz center frequency is used for the AOD's. The reference chirp is stored in a digitally programmable read only memory (PROM) and read out each laser diode trigger pulse using the CCD pixel clock and a digital-to-analog converter. Fig. 7(a) shows a reference chirp oscilloscope trace that was used in the experiments. The chirp, being digitally generated is perfectly coherent with the laser pulsing. Fig. 7(b) shows the Fourier plane optical spectra of a 3 MHz input tone and a 3.5 MHz amplitude modulated reference chirp. The DFT signal is generated by an IBM-PC image processing work station that is locked to the CCD detector clock. For video signal inputs, the CCD camera is locked to the CCD detector array by using special synchronizing circuitry. For folded spectrum processing of tones, the laser diode trigger frequency is adjusted according to the Nyquist criteria.

Experimental results from this processor are shown in Fig. 8 and 9 for a fine frequency analysis bandwidth of 7.86 KHz. The processor is operated with a coarse frequency resolution of 80 KHz per pixel. Data in Fig. 8 corresspond to a fine frequency variation from DC to 7.8 KHz with a zero coarse frequency variation. We see the



Downloaded From: https://www.spiedigitallibrary.org/conference-proceedings-of-spie on 07 Jun 2020
Terms of Use: https://www.spiedigitallibrary.org/terms-of-use

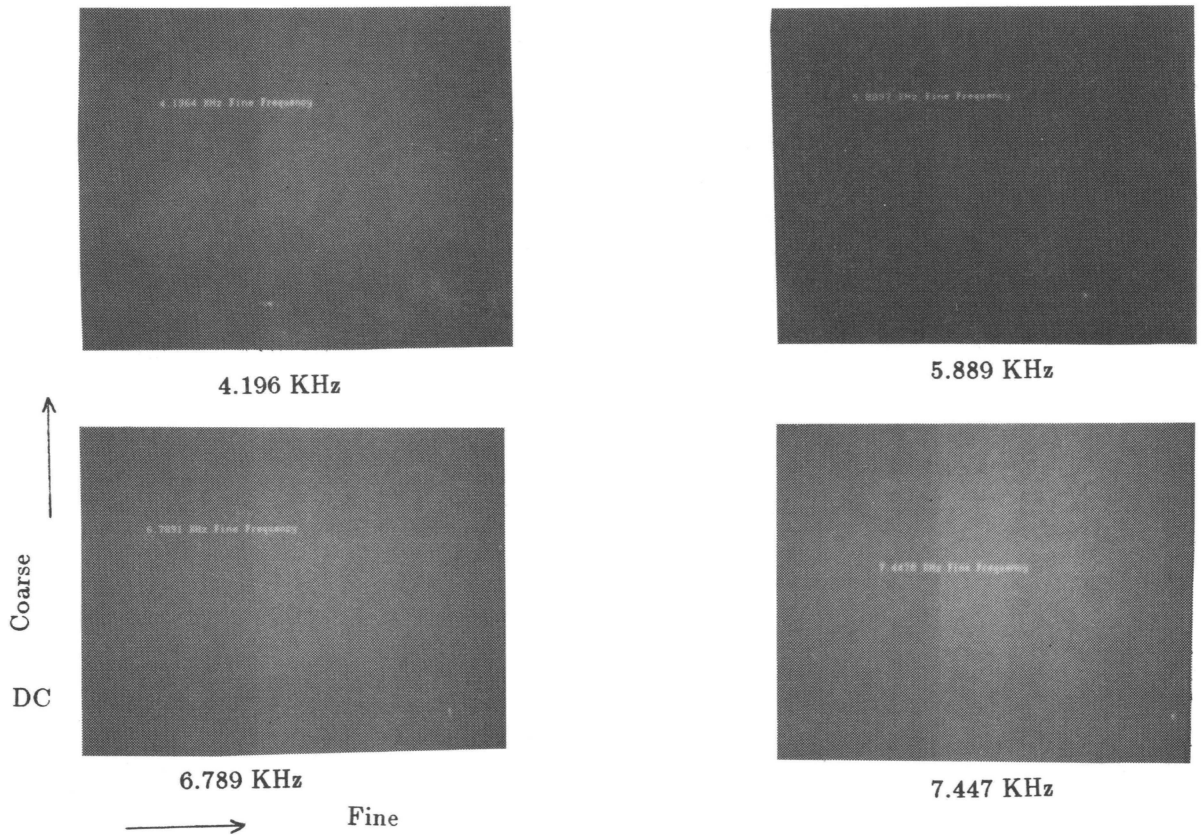



**Fig. 8** TSI Spectrum Analyzer Output for Fine Frequency Variation from DC -7.86 KHz

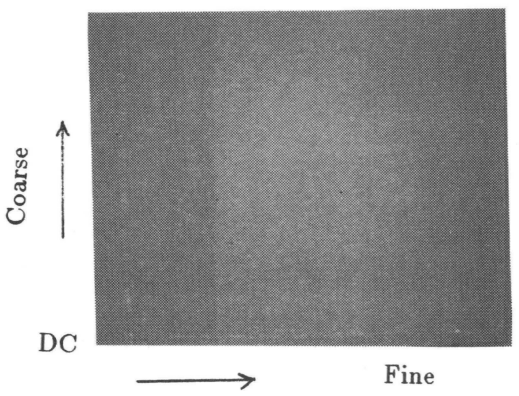



**Fig. 9(a)** Folded Spectrum Output for a 60.7179 MHz Single Tone Input

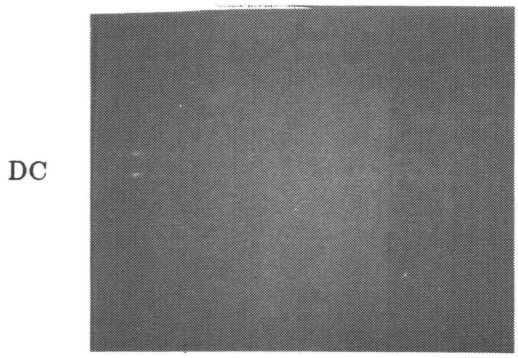



**Fig. 9(b)** 2-D Spectrum Output for a 623 KHz Tilted Grating Video Input

interference peak move from left(DC) to right(7.86 KHz) along the DC coarse frequency bin. Fig. 9(a) shows the 2-D folded spectrum of a single tone input where the position of the peak gives the coarse and fine frequencies. Coarse DC position corressponds to the base of the picture. Fig. 9(b) shows the 2-D video spectrum of a tilted grating used as the video image. The DC of the fast (coarse) variation along the x direction of the image corressponds to the central bin between the two peaks on the picture. The slow (fine) variation along the y direction of the image corressponds to the left to right movement of the peak along each fast frequency bin. We get two peaks instead of one because the video signal is mixed with 60 MHz before entering the Bragg cell giving an amplitud. modulatad signal whose spectrum has two sidebands located symmetrically around the 60 MHz carrier frequency. The single



Downloaded From: https://www.spiedigitallibrary.org/conference-proceedings-of-spie on 07 Jun 2020
Terms of Use: https://www.spiedigitallibrary.org/terms-of-use

tone experiments are carried out using a signal generator whose frequency is varied around 60 MHz. The 2-D results corresspond to spectrums after electronic bias subtraction.

## 5. Bias Removal Techniques

Bias separation from the desired signal is always an important issue in interferometric time integrating processors. We discuss three ways in which the bias can be removed. Pixel by pixel electronic bias subtraction can be done by using two synchonously operated CCD's, one to record the signal plus bias terms and the other for recording bias terms. This approach gives the real part of the spectrum only. In our experiments, we used a PC based image processing work station with a frame grabber to store the bias for subtraction. Another approach is to place the desired signal on a spatial carrier which is converted to a temporal variation by the natural readout mechanism of the CCD and then bandpass filtered by appropriate electronics. In the TSI processor, the 2-D spectrum can be placed on a spatial carrier by mixing the DFT signal with a frequency offsetted Bragg cell center frequency signal eg. 60.1 MHz and using a time delayed reference chirp signal. The bias subtraction and carrier demodulation methods of bias removal do not solve the problem of limited system dynamic range as processing is done after the detection of the signal. The effective system dynamic range at the output is

$$DR_s = DR[\frac{SBR}{(1+SBR)}]$$

where $DR$ is the dynamic range of the output detector (CCD) and $SBR$ is the signal to bias ratio on the detector. In most TI systems, $SBR$ is much less than one. One way of solving this dynamic range problem is by using a photorefractive crystal for bias removal.[7] The desired spectrum is generated on a spatial carrier and it is read out by a Bragg matched beam.

## 6. Processor Performance Issues

The Caltech processor shown in Fig. 6 achieved coarse and fine frequency resolutions of 80 KHz and 100 Hz respectively. The number of coarse and fine frequency resolution bins corressponded to 384 and 78 respectively. The bandwidth of the system is controlled by the bandwidth of the reference chirp which is programmed in a high speed PROM to 5 MHz for video signal inputs. Modulation depths of 30 percent were obtained. The performance is limited by nonuniformities in the reference chirp spectrum, the limited temporal coherence of the laser diode and intermodulation product terms resulting from AOD and amplifier nonlinearities. The coarse frequency resolution is limited by CCD pixel size, focal length of Fourier transforming lens, AO cell aperture and apodization effects. For the video processor, the ideal coarse frequency resolution of 15.7 KHz could be obtained by using a larger focal length lens and smaller CCD pixels. The fine frequency resolution is limited by the integration time of the CCD which is $1/60^{th}$ of a second, the CCD pixel size, the Bragg cell acoustic velocity and the imaging optics. Note that using carrier demodulation for bias removal reduces the number of frequency bins along the carrier direction.

## 7. Conclusion

We have demonstrated a multiplicative architecture for time and space integrating real time spectrum processing using AOD's as input transducers and CCD's as time integrating detectors. A Fourier transform lens is used to channelize the coarse frequency components while the time integrating DFT algorithm is used to resolve the fine frequency variation. Experimental data for the TI spectrum analyzer and TSI spectrum analyzer are given. The TSI system can be used as a folded spectrum processor for detecting 1-D time signals,eg. highly coherent narrowband signals buried in white noise. The system can also be used for spectrum analysis of video images. For example, texture analysis of Synthetic Aperture Radar (SAR) image returns for remote sensing applications can be done by cascading the optical SAR and TSI spectrum analyzer systems. This will also eliminate the need for expensive high speed analog-digital converter interface circuitry. In addition, the video processor can be used in pattern recognition applications such as real time security systems. Three bias removal schemes have been suggested including an optically efficient architecture using a photorefractive crystal as a time integrating detector. A later publication will discuss the details of this architecture and its experimental results. Note that because the architecture used is multiplicative in nature, it is common path and thus more stable to vibration than an additive architecture. Also, compared to an additive design, this architecture is simpler to build and align. Nevertheless, it has poorer light efficiency compared to the additive design. Future processor performance can be improved by using higher quality periphery electronic hardware and customized imaging optics.

## 8. Acknowledgements

We would like to thank Dr. Kelvin Wagner for many useful disscussions. This work was performed under grants from the Air Force Office of Scientific Research.



Downloaded From: https://www.spiedigitallibrary.org/conference-proceedings-of-spie on 07 Jun 2020
Terms of Use: https://www.spiedigitallibrary.org/terms-of-use

## Appendix A

This appendix gives the derivation of Eqn. 7 starting with Eqn. 6 given earlier.For simplicity of the analysis, we have assumed the $u = 0$ axis to corresspond to the position of the Bragg cell center frequency ($\omega_0$) on the CCD plane. The intensity on the $n_{th}$ pulse given in Eqn. 6 can be written as

$$I_n = |(S + C)(a + d)|^2 \tag{A1}$$

where '$S$' and '$C$' are Fourier spectrums of the information signal and reference chirps respectively taken by the space integrating Bragg cell spectrum analyzer and '$a$' and '$d$' are the reference bias signal and the spatially filtered and hetrodyned to baseband DFT signal respectively. '$a$' is a real quantity and '$d$' is given by

$$d = e^{-jn\frac{\Delta\omega}{v}y}$$

$$|d|^2 = 1$$

Using the above relations and expanding Eqn. A1 we get

$$\begin{aligned} I_n = {} & 2Re[aSC^*Re(d)] + (1 + a^2)|C|^2 + 2|C|^2Re(ad) \\ & + (1 + a^2)|S|^2 + 2|S|^2Re(ad) + 2(1 + a^2)Re(SC^*) \end{aligned} \tag{A2}$$

Note that the reference chirp is a perfectly coherent chirp with no dependence on $n$ as the same digital chirp is generated every laser diode pulse. $Re$ in Eqn. A2 stands for real value of a function. Eqn. A2 consists of 6 terms where the first term gives the 2-D spectrum, the second and third terms give the constant bias term and finally the fourth,fifth and sixth terms give the signal dependent bias term. Assuming the reference chirp spectrum $C$ is uniform over the information signal bandwidth and has an arbitary fixed phase which can be taken to be zero for simplicity of analysis, we can write $C = C_0$ where $C_0$ is a constant. Now taking the summation over all the $N$ laser diode pulses to find the charge distribution on the CCD, the first term in eqn. A2 gives

$$I_1 = 2aC_0Re[\sum_{n=0}^{n=N-1} SRe(d)] \tag{A3}$$

Substituting in Eqn. A3 the value of $S$ for a video signal and the value of $d$ , we get the desired 2-D spectrum

$$I_1(u, y) = KRe[\sum_{n=0}^{n=N-1} (\tilde{F}_n(u) * B(u)) \cos(\frac{n\Delta\omega}{v}y)] \tag{A4}$$

where $K$ is a constant term involving the constant terms $C_0$ and $a$ and the finite size of the CCD detector array in the $u$ and $y$ directions. We have used the blurr spot $B(u)$ to account for the finite aperture of the Bragg cell in the SI direction. The second and third terms of Eqn. A2 on summation give the constant bias term $K_1$ to be

$$K_1 = NC_0{}^2(1 + a^2) + 2aC_0{}^2 \cos(\alpha y)\frac{\sin(N\beta y)}{\sin(\beta y)} \tag{A5}$$

$$\alpha = (N - 1)\frac{\Delta\omega}{2v}$$

$$\beta = \frac{\Delta\omega}{2v}$$

where the first term in Eqn. A5 gives a constant bias level and the second term gives a fine frequency DC ridge along $y = 0$ with a very slow spatial modulation undetectable by the CCD. Now taking the summation over $n$ of the fourth,fifth and sixth terms in Eqn. A2, we get the signal dependent bias term $K_2$ as

$$K_2 = N(1 + a^2)|S(u)|^2 + 2a|S(u)|^2 \cos(\alpha y)\frac{\sin(N\beta y)}{\sin(\beta y)} + 2C_0(1 + a^2)|S(u)|a_1 \tag{A6}$$



Downloaded From: https://www.spiedigitallibrary.org/conference-proceedings-of-spie on 07 Jun 2020
Terms of Use: https://www.spiedigitallibrary.org/terms-of-use

Note that the absolute value operation on $S(u,n)$ in Eqn. A2 removes the time dependence in the spatial Fourier transform taken by the lens giving only the coarse frequency bias ridge terms in Eqn. A6. The first and third terms in Eqn. A6 give bias terms positioned at the signal coarse frequency ridges. The constant $a_1$ depends on the fine frequency of the signal. The second term gives the coarse frequency ridge crossed with the fine frequency DC ridge. Combining the results from equations A4, A5 and A6 we get the total time integrated charge distribution on the CCD to be

$$I(u,y) = KRe[\sum_{n=0}^{n=N-1} (\tilde{F}_n(u) * B(u)) \cos(n\frac{\Delta\omega}{v}y)] + K_1 + K_2 \qquad (A7)$$

The impulse response of the system for a video image input with a spatial frequency $u_0$ in the x-direction and spatial frequency $v_0$ in the y-direction of the image is

$$I_1 \approx \cos(\eta)\frac{\sin(N\gamma)}{\sin(\gamma)}[B(u-u_0) + B(u+u_0)] \qquad (A8)$$

$$\eta = (N-1)\gamma \approx \pi v_0 \Delta y(N-1)$$

$$\gamma = \pi v_0 \Delta y - \frac{\Delta\omega}{2v}y$$

where we used the fact that the modulation along y is slow. We will get two peaks positioned at the coordinates $u = u_0, y = 2\pi v_0 \frac{v\Delta y}{\Delta\omega}$ and $u = -u_0, y = 2\pi v_0 \frac{v\Delta y}{\Delta\omega}$.

For a single tone input signal with $f_c$ and $f_f$ the coarse and fine frequencies respectively, we get the impulse response of the system as

$$I_1 \approx \cos(\zeta)\frac{\sin(N\xi)}{\sin(\xi)}B(u - \frac{f_c}{v}) \qquad (A9)$$

$$\xi = \pi f_f T + \frac{\Delta\omega}{v}y$$

This time we get one peak located at $u = \frac{f_c}{v}, y = \pi f_f T \frac{v}{\Delta\omega}$ where $\zeta$ is a fine frequency dependent constant phase term.

## 9. References


[1] D. Psaltis and D. Casasent, "Time and Space Integrating Spectrum Analyzer," *Applied Optics*, vol. 18, p. 3203, 1979.

[2] T. R. Bader, "Acoustooptic Spectrum Analysis: a high performance hybrid technique," *Applied Optics*, vol. 18,No.10, May 1979.

[3] K. Wagner and D. Psaltis, "Time and Space Integrating Acousto-optic Folded Spectrum Processing for SETI," *Proc SPIE*, Vol 564-31, 1985.

[4] C. E. Thomas,"Optical Spectrum Analysis of Large Space Bandwidth Signals",*Applied Optics*, vol. 5, p. 1782, 1966.

[5] K. Wagner, "Time and Space Integrating Acousto-optic Signal Processing," Ph.D Thesis, California Institute of Technology, May 1987.

[6] T. M. Turpin,"Spectrum Analysis using Optical Processing," *Proc IEEE*,Vol 69. No1, January 1981.

[7] D. Psaltis, J. Yu and J. Hong, "Bias-free Time Integrating Optical Correlator using a Photorefractive Crystal," *Applied Optics*, vol. 24, No.22, Nov 1985.




Downloaded From: https://www.spiedigitallibrary.org/conference-proceedings-of-spie on 07 Jun 2020
Terms of Use: https://www.spiedigitallibrary.org/terms-of-use